

# Enhancement of photocatalytic activities of perovskite $\text{LaFeO}_3$ composite by incorporating nanographene platelets

N Afifah<sup>1,2</sup> and R Saleh<sup>1,2</sup>

<sup>1</sup>Department of Physics, Faculty of Mathematics and Natural Sciences Universitas Indonesia, Kampus UI Depok, Depok 16424, Indonesia

<sup>2</sup>Integrated Laboratory of Energy and Environment, Faculty of Mathematics and Natural Sciences Universitas Indonesia, Kampus UI Depok, Depok 16424, Indonesia

Corresponding author's e-mail: rosari.saleh@gmail.com

**Abstract.**  $\text{LaFeO}_3/\text{NGP}$  composites with several concentrations of NGP by weight percent were prepared using co-precipitation methods. The ferromagnetic behavior of  $\text{LaFeO}_3/\text{NGP}$  composites was characterized by vibrating sample magnetometer (VSM), while the structural properties were investigated using X-ray diffraction (XRD), Fourier transform infrared (FT-IR) spectroscopy, and Brunauer–Emmett–Teller (BET) surface area analysis. The  $\text{LaFeO}_3$  nanoparticles with and without NGP show orthorhombic structure and ferromagnetic behavior. The samples were used to degrade methylene blue using visible light irradiation. The obtained results revealed that the photocatalytic performance of  $\text{LaFeO}_3/\text{NGP}$  composites increased with increasing NGP from 3 wt.% up to 5 wt.%. The main factors influencing the photocatalytic activity were studied and are discussed herein.

## 1. Introduction

The carbon-based material graphene has attracted much attention because of its large specific surface area, flexible structure, excellent mobility of charge carriers, and good electrical and thermal conductivity [1-3]. Graphene, with its unique properties, could serve as a support material and dispersion medium for catalysts, which could inhibit the aggregation of catalyst while it is dissolving into aqueous organic dye [4-5]. The photocatalytic activity of graphene as a supporting material has been reported by several studies. Li *et al.* (2013) [6] and Morales-Torres *et al.* (2013) [2] reported the photocatalytic degradation of organic pollutants in wastewater by P25-graphene composite. Their results showed that the photocatalytic activity of P25-graphene composite is better than that of pure P25. Xiang *et al.* (2012) [7] and Tu *et al.* (2009) [8] also reported the photocatalytic activity of a graphene/ $\text{TiO}_2$  composite. The role of graphene in their composite is an electron transport channel, which could inhibit electron–hole recombination and enhance catalytic performance.

Graphene could support lanthanum ferrite ( $\text{LaFeO}_3$ ) nanoparticles as well as  $\text{TiO}_2$ .  $\text{LaFeO}_3$  is an  $\text{ABO}_3$  perovskite type-oxide that is widely used as a catalyst due to its unique optoelectronic properties and narrow optical band gap, making it suitable for application as a visible light photocatalyst [9, 10]. The photocatalytic activity of  $\text{LaFeO}_3$  nanoparticles was reported in our previous work [11]. However, in our previous studies,  $\text{LaFeO}_3$  nanoparticles could not completely degrade organic pollutants in the photocatalytic process. Therefore, in this research we combined nanographene platelets (NGP) with  $\text{LaFeO}_3$  in composite form to increase the photocatalytic performance.  $\text{LaFeO}_3/\text{NGP}$  with various weight percent (wt.%) of NGP were synthesized using the co-precipitation method. The photocatalytic activity of all samples was evaluated under visible light irradiation. Methylene blue (MB) was used as



a model organic pollutant. The stability of the catalyst and the main active species playing an important role in the photocatalytic process were also studied.

## 2. Experimental details

*Catalyst preparation:*  $\text{LaCl}_3 \cdot 7\text{H}_2\text{O}$ ,  $\text{FeCl}_2 \cdot 4\text{H}_2\text{O}$ , and sodium hydroxide (NaOH) were purchased from Merck (Kenilworth, NJ, USA). The chemical reagents were used to synthesis  $\text{LaFeO}_3$  nanoparticle based on our previous work [11]. Nanographene platelets (NGP), purchased from Angstrom Materials (Dayton, OH, USA), were then used to synthesis  $\text{LaFeO}_3/\text{NGP}$  composites using the co-precipitation method. The weight ratio of NGP to  $\text{LaFeO}_3$  varied at 3, 5, and 10 wt.%. Briefly, NGP was dissolved into 80 mL distilled water and 40 mL ethanol through ultrasonic treatment for 2 h. Then,  $\text{LaFeO}_3$  nanoparticles were added to the NGP solution, followed by stirring for 2 h. The suspension was then centrifuged and dried at  $70^\circ\text{C}$  for 12 h.

*Characterization:* The samples were characterized by X-ray diffraction (XRD), Fourier transform infrared (FT-IR), vibrating sample magnetometer (VSM), and Brunauer–Emmett–Teller (BET) surface area analysis spectroscopy.

*Photocatalytic activity:* The photocatalytic activity was determined by observing the degradation of MB under visible light irradiation. First, 0.4 g/L catalyst was dissolved into 100 mL of 20 mL/g MB. The resulting solution was stirred in the dark for 30 min to allow it to reach absorption–desorption equilibrium. Then, the suspension was irradiated using a 40 W Xe lamp as the visible light source for 2 h. The degradation of MB was monitored using a Hitachi (Tokyo, Japan) UH5300 UV-visible spectrophotometer. The degradation of MB was plotted as  $C_t/C_0$ , where  $C_t$  is the concentration of MB at each measurement interval during irradiation and  $C_0$  is the initial concentration of MB after reaching adsorption–desorption equilibrium. The stability of the catalyst was also checked in this research by reusing the catalyst for four times cycle processes. The main active species involved in the catalytic degradation of MB were studied using sodium sulfate, di-ammonium oxalate and tert-butyl alcohol, which are recognized as scavengers for electrons, holes, and hydroxyl radical species, respectively.

## 3. Results and discussion

The structural properties of all samples were characterized using XRD. Figure 1(a) shows the XRD pattern of the  $\text{LaFeO}_3/\text{NGP}$  composites with different wt.% NGP. The XRD pattern of  $\text{LaFeO}_3$  nanoparticles is also shown as a comparison. The diffraction peak at  $2\theta$  of  $26.4^\circ$  confirmed the graphite structure of NGP. The obtained diffraction peak of NGP increased with increasing wt.% NGP. The orthorhombic structure of  $\text{LaFeO}_3$  could also be found in the XRD pattern of all composites. No other phases or impurities were found, indicating that the desired synthesized sample was obtained. Along with XRD measurements, the crystal size value could also be calculated using Scherrer's formula [12]. The crystal size and lattice parameters of all samples are summarized in table 1.

The incorporation of NGP into the composite was confirmed by FT-IR measurements. Figure 1(b) shows the FT-IR spectra of the  $\text{LaFeO}_3/\text{NGP}$  composites with various wt.% NGP. The FT-IR spectrum of pure NGP is also shown for comparison. The strong absorption at wavenumber  $555\text{ cm}^{-1}$  is the Fe–O stretching vibration of octahedral  $\text{FeO}_6$ , which was characteristic of the material forming the perovskite  $\text{LaFeO}_3$  [12–14], while the C=O stretching vibration at  $1460\text{--}1750\text{ cm}^{-1}$  confirmed the presence of NGP in the sample [15–16]. The O–H stretching vibration was also found at wavenumber  $3440\text{ cm}^{-1}$  [16].

Magnetic saturation of the  $\text{LaFeO}_3$  nanoparticles and  $\text{LaFeO}_3/\text{NGP}$  composites with various wt.% NGP can also be seen in figure 1(c). All samples showed ferromagnetic behavior at room temperature. The magnetic saturation of the composite increased as the wt.% of NGP increased up to 5 wt.%. The magnetic saturation of  $\text{LaFeO}_3/\text{NGP}$  composites is summarized in table 1.

The photocatalytic activity of the  $\text{LaFeO}_3/\text{NGP}$  composites with various wt.% NGP is shown in figure 2(a). In comparison, the photocatalytic activity of  $\text{LaFeO}_3$  nanoparticles is also shown. The results showed that the degradation of MB increased with the addition of NGP up to 5 wt.% and then decreased with the addition of 10 wt.% NGP. The degradation rate of MB was also calculated using the pseudo-

first-order kinetic rate equation [17]. The obtained result (shown in figure 2(b)) revealed that  $\text{LaFeO}_3$

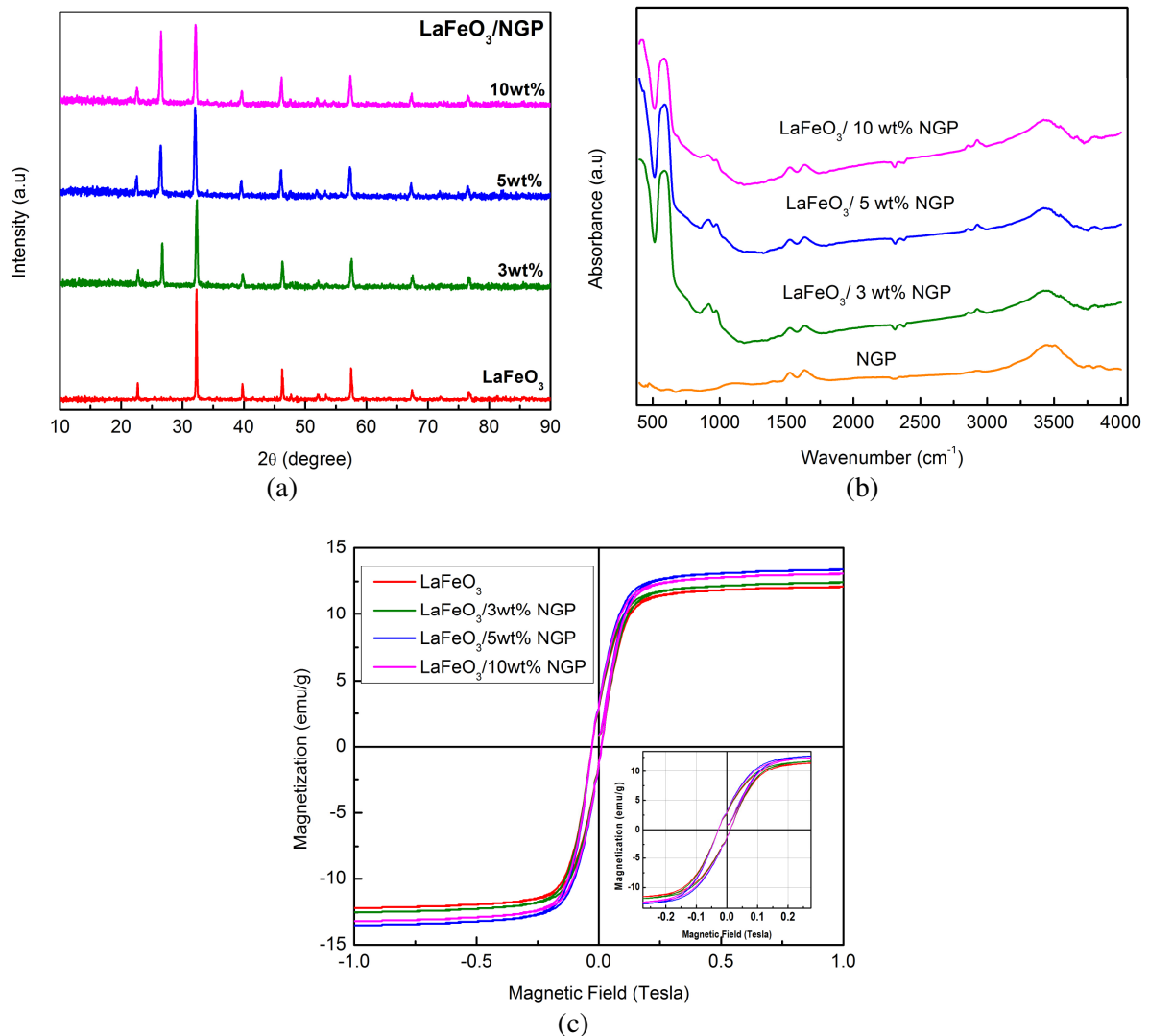


**Figure 1.** (a) XRD pattern; (b) FTIR spectra; and (c) VSM spectra of  $\text{LaFeO}_3/\text{NGP}$  composites with different wt.% NGP.

**Table 1.** The lattice parameter, grain size  $\langle D \rangle$ , magnetic saturation (M-S) and surface area of  $\text{LaFeO}_3/\text{NGP}$  composites.

Sample	Lattice Parameter			$\langle D \rangle$ (nm)	M-S (emu/g)	Surface area (eV)
	a (Å)	b (Å)	c (Å)			
$\text{LaFeO}_3$	5.5436	7.8456	5.5528	58	12.08	-
$\text{LaFeO}_3/3 \text{ wt.}\% \text{ NGP}$	5.5326	7.8376	5.5592	28	12.41	43
$\text{LaFeO}_3/5 \text{ wt.}\% \text{ NGP}$	5.5632	7.8687	5.5727	27	13.38	76
$\text{LaFeO}_3/10 \text{ wt.}\% \text{ NGP}$	5.5703	7.8782	5.5743	28	13.06	90

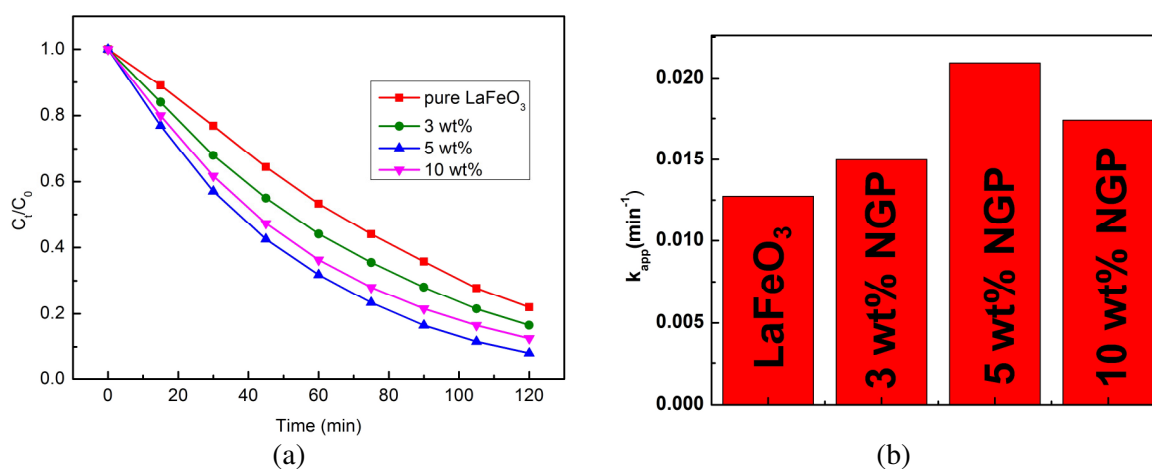


**Figure 2.** (a) The photocatalytic activity of LaFeO<sub>3</sub>/NGP composites with various wt.% NGP; and (b) The degradation rate of MB using LaFeO<sub>3</sub>/NGP composites with various wt.% NGP.

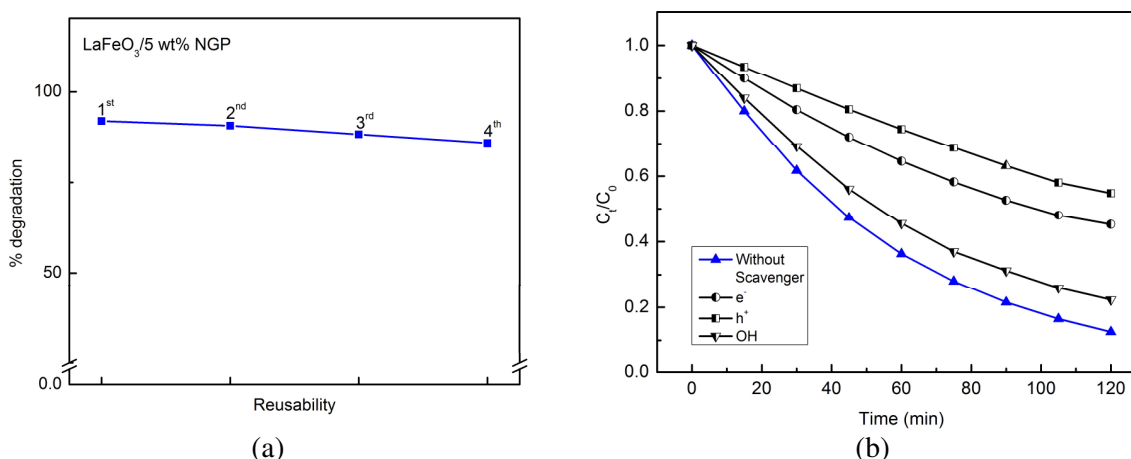


**Figure 3.** (a) The stability of catalyst using LaFeO<sub>3</sub>/5 wt.% NGP; and (b) The effect of scavengers on photocatalytic degradation of MB using LaFeO<sub>3</sub>/5 wt.% NGP.

with added NGP shows more rapid degradation of MB than LaFeO<sub>3</sub> without NGP. It has been suggested that the photocatalytic efficiency depends on several factors, one of which is surface area. A large surface area may increase the opportunity for contact between the catalyst and light, thereby increasing the rate at which the oxidation process happens [18]. The surface area of the LaFeO<sub>3</sub>/NGP composites is summarized in table 1. The results show that increasing the NGP content increased the surface area of the catalyst. However, the highest photocatalytic activity was observed with 5 wt.% added NGP. This indicates that the photocatalytic degradation efficiency of the composite was more influenced by the capacity of the electron transport layer of NGP, which could inhibit electron-hole recombination and enhance photocatalytic performance [18-20].

After determining the catalyst with the maximum degradation rate, the stability of the catalyst was also observed. MB solutions were degraded using the same catalyst four times under the same treatment conditions. The results of reusing the LaFeO<sub>3</sub>/NGP composite (5 wt.%) as a catalyst can be seen in figure 3(a). After four repetitions, the catalyst did not show a significant decrease in activity, indicating that the catalyst has good stability.

To study the main active species in the process of MB degradation using the LaFeO<sub>3</sub>/NGP composite (5 wt.%), the experiment was repeated with the addition of active species like electrons, holes, and

hydroxyl radicals.  $\text{Na}_2\text{S}_2\text{O}_8$  and di-ammonium oxalate were used as electron and hole scavengers, while tert-butyl alcohol was used as a hydroxyl radical scavenger. The influence of these scavengers on the photocatalytic activity of  $\text{LaFeO}_3/\text{NGP}$  composites (5 wt.%) is shown in figure 3(b). The presence of scavengers decreased the degradation rate of MB; the largest decrease was obtained with di-ammonium oxalate. This result indicates that the holes play the most important role in the photocatalytic activity.

#### 4. Conclusions

The photocatalytic activity of  $\text{LaFeO}_3/\text{NGP}$  composites with various wt.% NGP has been investigated under visible light irradiation. The composite with incorporated NGP shows better photocatalytic performance than the  $\text{LaFeO}_3$  nanoparticles. The  $\text{LaFeO}_3/\text{NGP}$  composites also showed stability as they were able to degrade MB through four photocatalytic cycles without a decrease in efficiency. The role of NGP in composites could inhibit electron-hole recombination and enhance catalytic performance.

#### References

- [1] Aleksandrak M, Adamski P, Kulka W, Zielinska B and Mijowska E 2015 *Appl. Surf. Sci.* **331** 193-9
- [2] Morales-Torres S, Pastrana-Martínez L M, Figueiredo J L, Faria J L and Silva A M 2013 *Appl. Surf. Sci.* **275** 361-8
- [3] Machado B F and Serp P 2012 *Catal. Sci. Technol.* **2** 54-75
- [4] Zhou K, Zhu Y, Yang X, Jiang X and Li C 2011 *New J. Chem.* **35** 353-9
- [5] Liang D, Cui C, Hu H, Wang Y, Xu S, Ying B, Li P, Lu B and Shen H 2014 *J. Alloy. Compd.* **582** 236-40
- [6] Li J, Zhou S, Hong G and Chang C 2013 *Chem. Eng. J.* **219** 486-91
- [7] Xiang Q, Yu J and Jaroniec M 2012 *Chem. Soc. Rev.* **41** 782-96
- [8] Tu W, Zhou Y, Liu Q, Yan S, Bao S, Wang X, Xiao M and Zou Z 2009 *Adv. Funct. Mater.* **19** 894-904
- [9] Grabowska E 2016 *Appl. Catal. B: Environ.* **186** 97-126
- [10] Tang P, Tong Y, Chen H, Cao F and Pan G 2013 *Curr. Appl. Phys.* **13** 340-3
- [11] Afifah N and Saleh R 2016 *J. Phys. Conf. Ser.* **710** 012030
- [12] Abazari R and Sanati S 2013 *Superlattice. Microst.* **64** 148-57
- [13] Noroozifar M, Khorasani-Motlagh M, Ekrami-Kakhki M S and Khaleghian-Moghadam R 2014 *J. Power Sources* **248** 130-9
- [14] Kaiwen Z, Xuehang W, Wenwei W, Jun X, Siqi T and Sen L 2013 *Adv. Powder Technol.* **24** 359-63
- [15] Fujii T, Matsusue I, Nakatsuka D, Nakanishi M and Takada M 2015 *Mater. Chem. Phys.* **129** 805-9
- [16] Taufik A and Saleh R 2016 *AIP Conf. Proc.* **1725** 020089
- [17] Saleh R and Djaja N F 2014 *Superlattice. Microst.* **74** 217-33
- [18] Kim T W, Park M, Kim H Y and Park S J 2016 *J. Solid State Chem.* **239** 91-8
- [19] Hu J, Men J, Ma J and Huang H 2014 *J. Rare Earth.* **32** 1126-34
- [20] Hu J, Ma J, Wang L and Huang H 2014 *J. Alloy. Compd.* **583** 539-45